ELSEVIER

Marine Geology 153 (1999) 239–252

MARINE GEOLOGY
INTERNATIONAL JOURNAL OF MARINE GEOLOGY, GEOCHEMISTRY AND GEOPHYSICS

Mediterranean planktonic foraminiferal faunas during the last glacial cycle

A. Hayes [a], E.J. Rohling [a,*], S. De Rijk [a], D. Kroon [b], W.J. Zachariasse [c]

[a] *Department of Oceanography, Southampton University, Southampton Oceanography Centre, European Way, Southampton, Hampshire SO14 3ZH, UK*
[b] *Department of Geology and Geophysics, University of Edinburgh, Edinburgh EH9 3JW, UK*
[c] *Department of Geology, Institute of Earth Sciences, Utrecht University, P.O. Box 80021, 3508 TA Utrecht, Netherlands*

Received 30 May 1997; accepted 3 February 1998

Abstract

This paper highlights the planktonic foraminiferal abundance variations during the last glacial cycle from six new cores along a roughly west–east transect in the Mediterranean Sea, together with results from previous studies. Multivariate statistical analysis describes a first significant axis that indicates a general sea surface temperature (SST) gradient from west to east. As expected lower SST values are recorded in glacial times but the eastern and western basins seem to have reacted differently to glacial conditions. The western basin shows a SST decrease from the Alboran Sea to the central Mediterranean, whereas the eastern basin records a west to east increase that is similar to the present-day eastern Mediterranean gradient. These new results show that: (1) few almost basin-wide faunal trends may be recognised, but these are interrupted by local anomalies with opposing trends; and (2) major abundance variations are distinctly diachronous in some species and virtually synchronous in others. The implication is that over the glacial–interglacial timescale concerned, biostratigraphy should only be used on a local rather than basin-wide scale, unless it is supported by other independent dating methods.

Keywords: biostratigraphy; palaeo-sea surface temperature; palaeoclimatology; oxygen isotope stratigraphy; Mediterranean

1. Introduction

The only connection of the present-day Mediterranean Sea to the open ocean consists of the Strait of Gibraltar. The Strait of Sicily divides the Mediterranean into the main western and eastern basins, while several satellite basins may be distinguished in more detail, such as the Aegean, Adriatic and Alboran seas (Fig. 1). The Mediterranean Sea is dominated by an excess of evaporation over freshwater input resulting in strong temperature and salinity gradients in surface waters from west to east (e.g. Wüst, 1961). The most notable contrasts are found between the western and eastern basins, on either side of the Strait of Sicily. The gradients are thought to exert the main control on planktonic foraminiferal distribution patterns (e.g. Thunell, 1978; Pujol and Vergnaud-Grazzini, 1995), in which case temporal variations in the gradients should be expressed by changes in the faunal assemblages.

Planktonic foraminifera in the Mediterranean Sea

* Corresponding author. Fax: +44 (1703) 593059; E-mail: e.rohling@soc.soton.ac.uk

0025-3227/99/$ – see front matter
PII: S0025-3227(98)00019-X

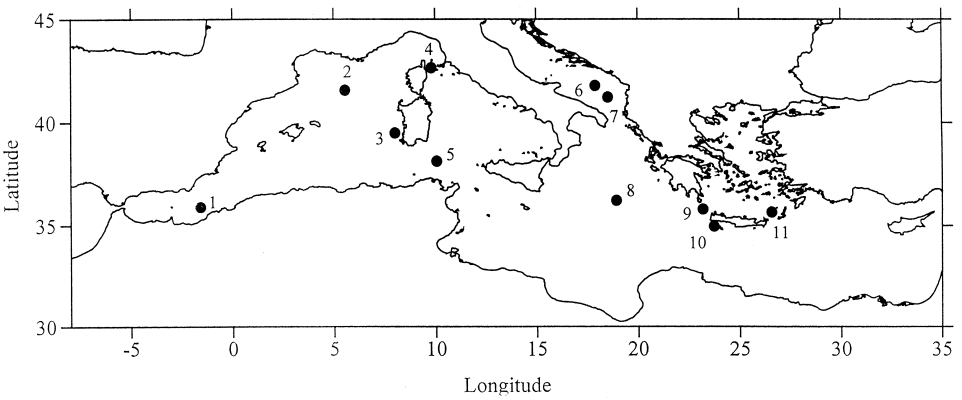

Fig. 1. A map of the Mediterranean Sea illustrating core localities. For reference to sub-basins see Rohling and De Rijk (1999).

have been extensively studied since the first piston cores were taken during the Swedish Deep Sea Expedition of 1946–47 (e.g. Kullenberg, 1952; Todd, 1958; Parker, 1958; Olaussen, 1960, 1961; Herman, 1972; Cita et al., 1977; Thunell et al., 1977; Vergnaud-Grazzini et al., 1977; Thunell, 1978, amongst others). In the western Mediterranean previous work on long cores primarily concerned oxygen isotope results rather than faunal variations (Paterne et al., 1986; Vazquez et al., 1991), while studies concerned with faunal abundances concentrated on the last deglaciation (e.g. Pujol and Vergnaud-Grazzini, 1989; Rohling et al., 1995). Meanwhile, the presence in the eastern Mediterranean of dark coloured, organic-rich sediments (sapropels) deposited intermittently throughout the late Cenozoic (Cita et al., 1973), has resulted in the concentration of studies using planktonic foraminiferal records on the palaeoecological and palaeoclimatic changes occurring specifically around periods of sapropel deposition (among many others, Thunell et al., 1977; Thunell and Williams, 1983; Ganssen and Troelstra, 1987; Tang and Stott, 1993; Rohling et al., 1997). Comparatively few studies reported on the general faunal development in the eastern Mediterranean over the last interglacial/glacial cycle (e.g. Cita et al., 1977; Buckley et al., 1982; Thunell and Williams, 1983; Rohling and Gieskes, 1989; Rohling et al., 1993). A comprehensive study of several long cores from the Strait of Sicily led Muerdter and Kennett (1984) to propose a generalised pattern of species abundance variations over the last seven isotope stages.

We here present a comparison of planktonic foraminiferal fauna variations in eleven long cores from various locations through the Mediterranean along a west–east transect (Fig. 1). The objective is to establish correlations between these cores and then to: (1) assess the applicability of planktonic foraminiferal biostratigraphy, such as that proposed by Muerdter and Kennett (1984), to basin-wide scales; and (2) present our main faunal results in such a manner that they may assist area-specific correlations in future faunal studies. Finally, we present results from the first significant axis obtained in multivariate statistical analysis (standardised Principal Components Analysis, PCA) of the entire data-set, which subdivides the faunal patterns in a surprisingly similar way to previous multivariate analyses performed on more limited data-sets (Thunell, 1978; Rohling et al., 1993). We plot the scores on that axis for all cores of our transect to evaluate the temporal variations of the W–E faunal gradients during the last interglacial/glacial cycle.

2. Materials and methods

Eleven sediment cores are used in this study: five from the western Mediterranean and six from the eastern Mediterranean. Details and core locations are summarised in Table 1 and Fig. 1. Previous work provided data for: (1) the upper 2 m of core KS310 (Rohling et al., 1995), and we here include results for the remaining sections down to 9.5 m; (2) core BS78-12 (Jorissen et al., 1993); (3) IN68-9 (Jorissen et al., 1993, resolution increased by Rohling et al.,

Table 1
Summary of the core details referred to in this paper

Core name	Region	Long.	Lat.	Water depth (m)	Cruise	Core length (cm)	AMS ^{14}C	Oxygen isotopes
KS310	Alboran Sea	1.57ºW	35.55ºN	1900	Faegas	940	No	No
BC15	Gulf of Lions	5.56ºE	41.57ºN	2500	Marion Dufresne	600	Yes (3)	*N. pachyderma* (1)
LC03	West Sardinia	8.01ºE	39.05ºN	423	Marion Dufresne 81	500	No	*N. pachyderma* (2)
BS78-12	Tyrrhenian Sea	9.81ºE	42.66ºN	626		552	Yes (3)	No
LC07	Western Sicily Strait	10.07ºE	38.14ºN	488	Marion Dufresne 81	420	No	*N. pachyderma* (2)
IN68-9	Adriatic Sea	17.09ºE	41.79ºN	1234	Van Straaten	609	Yes (3)	*G. bulloides* (3)
IN68-5	Adriatic Sea	18.53ºE	41.23ºN	1030	Van Straaten	643	Yes (3)	*G. bulloides* (3)
P4	Ionian Sea	18.93ºE	36.23ºN	3560	Discovery	340	No	No
T87/2/27G	N. Levantine Basin	23.02ºE	35.08ºN	607	Tyro	300	Yes (3)	No
T87/2/20G	N. Levantine Basin	23.74ºE	35.97ºN	707	Tyro	280	Yes (3)	*G. ruber* (3)
LC21	NE Crete	26.58ºE	35.66ºN	1522	Marion Dufresne 81	350	No	No

(1) = Stable Isotope Laboratory, University of California, Santa Cruz, USA; (2) = Stable Isotope Laboratory, University of Edinburgh, UK; (3) = Stable Isotope Laboratory, University of Utrecht, Netherlands.

1997); (4) IN68-5 (Jorissen et al., 1993); (5 and 6) T87-2-20G and 27G (Rohling et al., 1993).

All micropalaeontological samples were dried at 50ºC, weighed for total sample dry weight, then disaggregated in demineralised water, wet sieved through mesh diameters of 600, 150, 125 and 63 μm while rinsing with demineralised water, and finally dried and weighed to obtain a dry weight per sieve fraction. Planktonic foraminifera in the 150–600 μm size fraction were counted from suitable aliquots of approximately 200 specimens obtained using a random splitter. All specimens were identified and mounted in Chapman slides, and the counting results are expressed in terms of relative (%) and absolute (g^{-1}) abundances. We here present relative abundance data.

AMS ^{14}C dates were available for six of the cores (Table 1 with source-citations). In addition to previously obtained oxygen isotope records (IN-68-9, Rohling et al., 1997; IN68-5, Jorissen et al., 1993; T87-2-20G, Rohling et al., 1993), we present new records for western Mediterranean cores BC15, LC03, and LC07, based on samples of 20–30 hand-picked specimens of *N. pachyderma* (right-coiling) from the 250 to 350 μm size range as determined with an ocular micrometer (Table 1; Fig. 2).

3. Time stratigraphic frameworks

In addition to the oxygen isotope stratigraphic data (Fig. 2) and AMS ^{14}C dates (Table 2) for a number of the cores, additional datings were obtained using lithostratigraphic (ash layers, sapropel boundaries) and biostratigraphic correlations to dated cores from the same area (Fig. 2). All AMS ^{14}C dates were converted into calendar years using program Calib 3.03 (Stuiver and Reimer, 1993) with calibration data-set 3 and $\Delta R = -135$ ^{14}C yr (Stuiver and Braziunas, 1993), to enable direct comparison with the (orbitally tuned = calendar year) ages for isotopic events after Martinson et al. (1987). For the construction of calendar age–depth plots (Fig. 3), we subtracted all thicknesses of turbidites and ash layers from core depths, thus assuming that these layers were deposited geologically instantaneously. Using the average sedimentation rates (Fig. 3), the approximate position of the main isotopic events in cores lacking an isotope record could be found through inter-/extrapolation, based on the ages of these events after Martinson et al. (1987). The approximate depths derived in this manner (Table 2) are used to indicate the isotopic stages for these cores lacking their own isotope record (Fig. 4). The original age of 12,050 cal. BP for isotope event 2.0 (Martinson et al., 1987) is not used; instead we use the AMS ^{14}C based age for that event which is

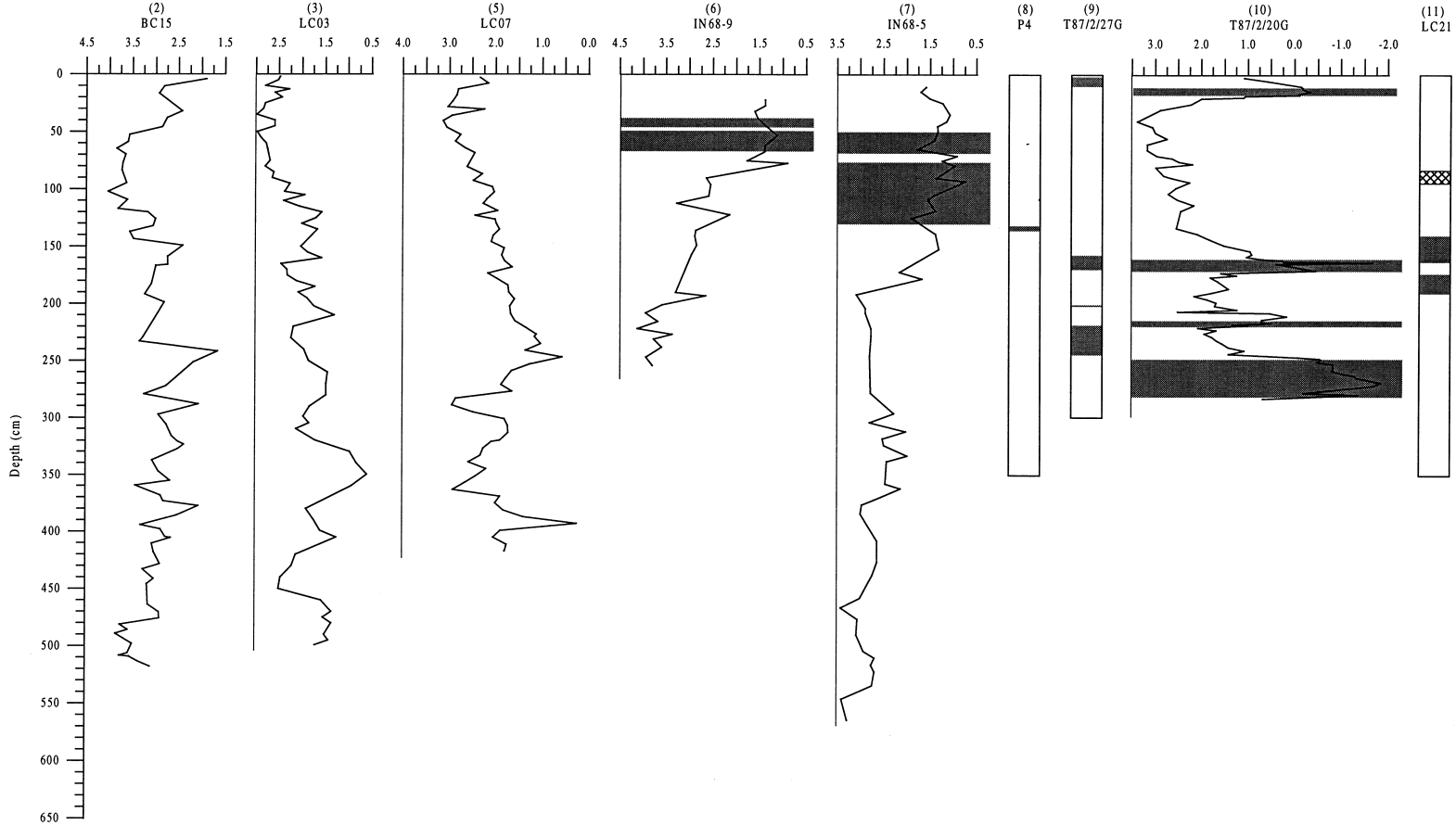

Fig. 2. Oxygen isotope records for select cores (see Table 1) and lithostratigraphic horizons used as dating control points. Numbers in brackets refer to core localities illustrated in Fig. 1.

equivalent to about 11,000 cal. BP (e.g. Jorissen et al., 1993).

4. Results

4.1. Faunal results

The planktonic foraminiferal results for the main species discussed in this paper are shown in Fig. 4 (complete faunal data are available on request). Although *Globigerina bulloides* is present in significant numbers (20–60%) in all of the eleven cores, its abundance variations are highly variable and so of little significance for correlation purposes. Also *G. bulloides* does not commonly feature on the first significant axis multivariate statistical analyses (cf. Thunell, 1978; Rohling et al., 1993; this paper), and so does not influence our interpretation of temporal changes in the W–E faunal gradient through the Mediterranean. Neither does *Globigerinita glutinata* feature in the multivariate analyses, and its biostratigraphic potential is found to be limited to local peak to peak correlations, e.g. in the Adriatic Sea (Jorissen et al., 1993) and Alboran Sea (Pujol and Vergnaud-Grazzini, 1989). On the basis of these arguments, we have decided to omit the graphs with the abundance variations of these two taxa, in spite of their generally significant presence.

For reasons explained by Rohling et al. (1993) the species *Globigerinella siphonifera*, *Hastigerina pelagica*, *Globoturborotalita rubescens*, *Orbulina universa*, *Globigerina digitata*, *Globoturborotalita tenella* and *Globigerinoides sacculifer* have been assembled into one entity, named the SPRUDTS-group. These individually rare species consistently group together in multivariate analyses (Thunell, 1978; Rohling et al., 1993; this study).

We observe a general consistency in the fluctuations of *Globigerinoides ruber* (Fig. 4a), with a major peak abundance in the middle of isotope stage 1 that is obvious in all records containing this interval. Also the main increase associated with the stage 2/1 boundary is fairly uniform as is the preceding minor increase in the upper part of stage 2. The stage 6/5 boundary increase in *G. ruber* is also a relatively common and well discernable feature. Exceptions to these general patterns are found in cores KS310 (Alboran Sea) and LC03 (west of Sardinia), where little variability is observed in *G. ruber* abundances.

The SPRUDTS-group tends to follow the pattern established by *G. ruber* in stage 1 and its increase is remarkably synchronous along the transect. Similarly most records show a near synchronous rapid increase at the stage 6/5 boundary.

The exit of *Globorotalia scitula* between late stage 2 and early stage 1 is a clearly diachronous event. In western (except Alboran Sea) and Adriatic Sea cores, *G. scitula* shows a strong decline well before the stage 2/1 boundary, whereas it continues well into stage 1 in more eastern cores, even if it is generally less abundant.

In contrast to *G. scitula*, *Turborotalita quinqueloba* shows a much more synchronous disappearance along the entire transect with respect to the stage 2/1 boundary. Numbers decrease from approximately 25% in stage 2 to $<10\%$ at the boundary prior to a minor peak in the lower part of stage 1.

The applicability of basin-wide single (key) species correlation is seriously questioned with the fluctuations of *Globorotalia inflata*. In NW Mediterranean core BC15, and Levantine cores T87-2-27G and T87-2-20G, *G. inflata* disappears in the upper part of stage 3 and reappears around mid-stage 2; a pattern which corresponds well to that observed by Muerdter and Kennett (1984). A similar pattern occurred in early stage 5 of the Levantine cores (Fig. 4e). However, in LC07 (west of Strait of Sicily) *G. inflata* numbers are reduced in the upper stage 3–lower stage 2 interval but the species never disappears. The same interval in core LC03 records similar distribution patterns, although the stage 3/2 boundary observes a temporary increase of *G. inflata* numbers. In the Alboran Sea, *G. inflata* behaves completely different from the rest of the Mediterranean, in that it reaches its highest peak in stage 1. This has been described to local hydrography, namely the development and continued presence of a frontal system since about 9000 cal. BP (Rohling et al., 1995).

4.2. Principal component analysis

Standardised Principal Components Analysis (PCA) is performed on the combined records of

Table 2
AMS ^{14}C dating points

Core	Depth of AMS ^{14}C dates (cm)	AMS ^{14}C dates	Calendar years ka BP	2.0 11,000 ka BP	3.0 24,100 ka BP	4.0 59,000 ka BP	5.0 73,900 ka BP	6.0 129,800 ka BP	7.0 189,600 ka BP
KS310 (1)	64.0		8,300	108	304	825			
	86.0		9,000						
	108.0		10,700						
	132.0		13,000						
	155.0		14,500						
	170.0		15,000						
	187.0		16,000						
BC15	4.25	10, 150 ± 800	11,200	0	126	481			
	64.75	14, 670 ± 900	17,300						
	175.25	27, 380 ± 240	30,200						
	256.25	31, 600 ± 400	34,400						
LC03				0	106	407			
BS78-12	50.0	4, 140 ± 80	4,400	171					
	85.0	7, 120 ± 80	7,700						
	147.25	10, 600 ± 200	12,200						
	282.75	13, 820 ± 190	16,200						
	551.25	21, 100 ± 400	24,300						
LC07				12	40	114	146	265	393
IN68-9	7.50	3, 160 ± 120	3,100	107					
	38.50	6, 390 ± 60	7,000						
	81.25	9, 280 ± 180	10,000						
	157.50	13, 100 ± 200	15,200						
	201.50	14, 200 ± 300	16,700						
	247.50	17, 200 ± 300	20,000						
IN68-5	11.0	5, 800 ± 100	6,300	196					
	158.0	9, 870 ± 170	10,900						
	292.0	11, 900 ± 300	13,600						
	418.0	13, 700 ± 300	16,100						
	566.0	14, 700 ± 300	17,300						
P4 (2)	87.0		6,900	170					
	135.0		9,000						
	145.0		9,800						
	240.0		14,600						
T87/2/27G	70.0	29, 800 ± 700	32,600	21	47	116	145	255	
	86.5	35, 100 ± 1400	37,900						
T87/2/20G	21.0	11,680	13,300	21	49	125	157	279	
	37.50	15,640	18,300						
	71.0	26,100	28,900						
LC21 (2)	95.0		3,650	264					
	139.0		7,000						
	189.0		9,000						
	223.0		9,300						
	258.0		10,600						
	335.0		13,800						

Dates were not obtained for cores KS310, P4 and LC21, although local biostratigraphy provided correlation with dated records: (1) = Pujol and Vergnaud-Grazzini (1989) (see Rohling et al., 1995); (2) = Jorissen et al. (1993). The right-hand side of the table illustrates isotope events from Martinson et al. (1987), used to provide a boundary depth (cm) of each event in each core by means of inter-/extrapolation.

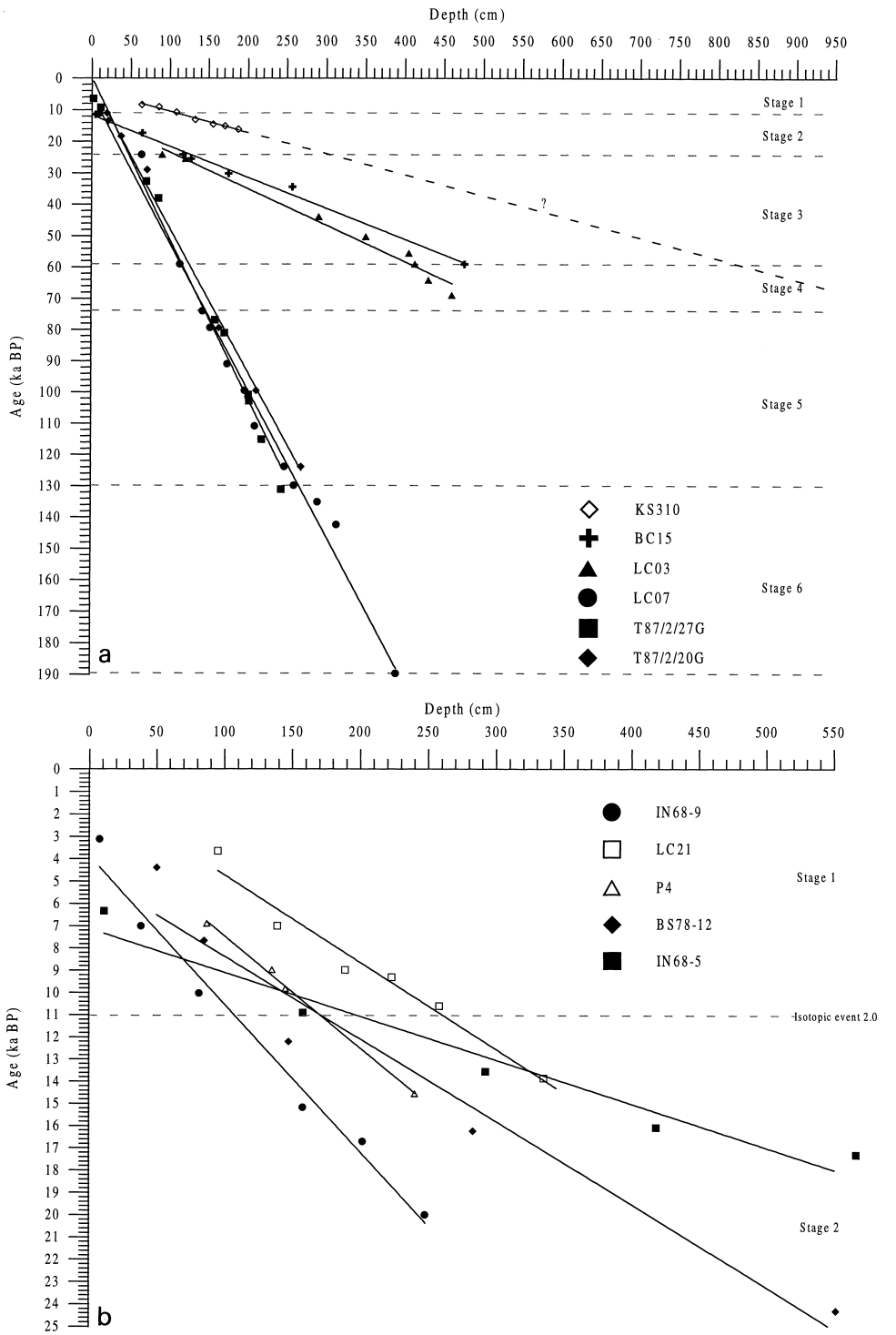

Fig. 3. Age–depth plots: (a) cores containing *only* isotope stages 1 and 2; (b) cores containing isotope stages 1–7. All ages are in calendar years (see Table 2). Depth is measured from the core top (= 0 cm) and all ash layers and turbidites have been extracted. Black symbols correspond to cores that have been dated by AMS ^{14}C dates whereas white symbols represent cores that are biostratigraphically dated. Grey dashed lines depict isotope stage boundaries. Only core KS310 has been significantly extrapolated to a depth of 950 cm and is illustrated by a dot–dash line. All linear fits have a R^2 coefficient >0.95.

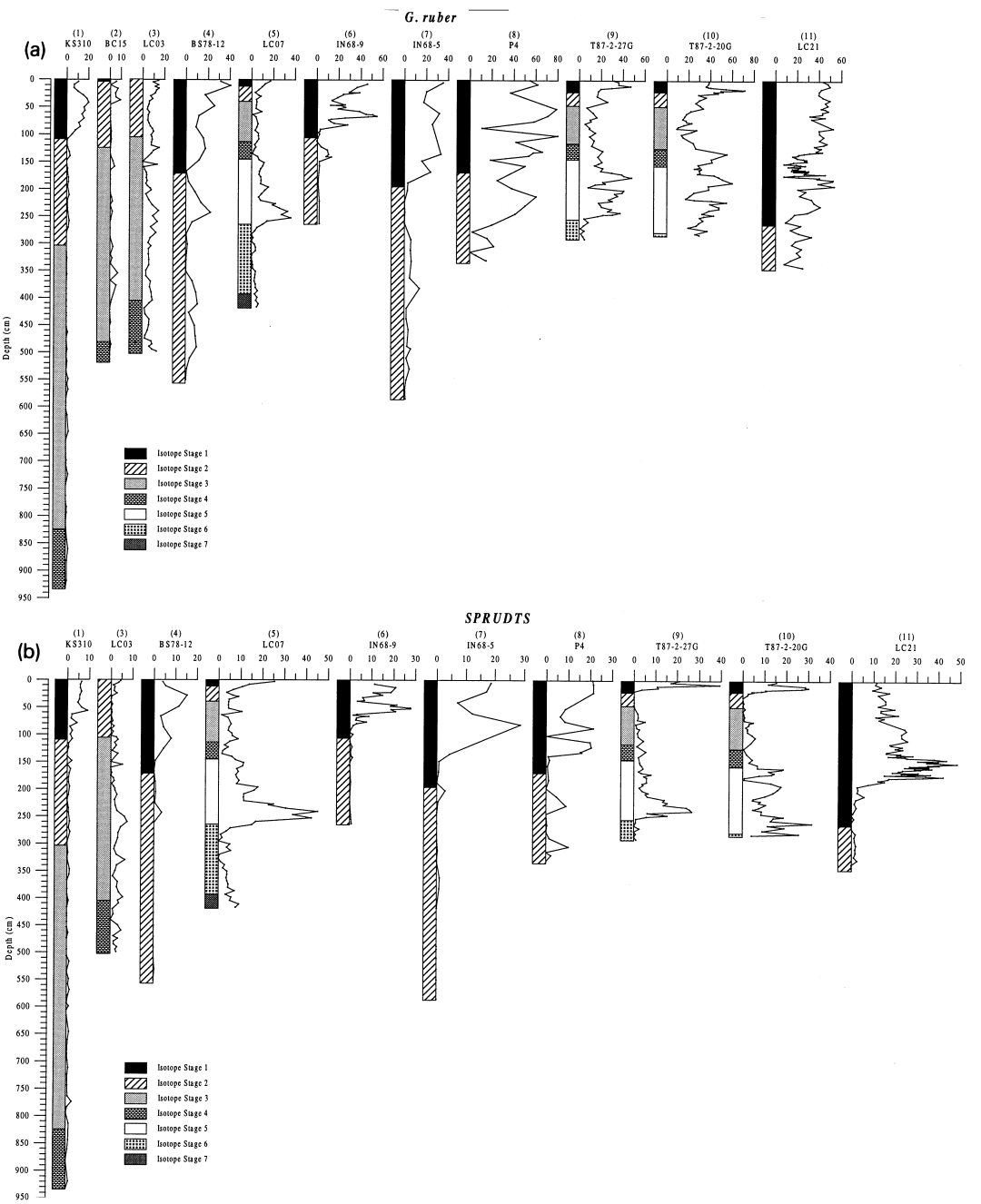

Fig. 4. (a–f). Planktonic foraminiferal percentages versus core depth, for the significant species along the west–east transect. Numbers in brackets refer to the core localities illustrated in Fig. 1.

all eleven cores in the transect (640 samples). The first component (PC1), describing 27.4% of the total variance is shown in Table 3, showing high positive loadings of *G. ruber* and the SPRUDTS-group versus high negative loadings of *T. quinqueloba*, *G. scitula*, *G. inflata* and *Neogloboquadrina pachy-*

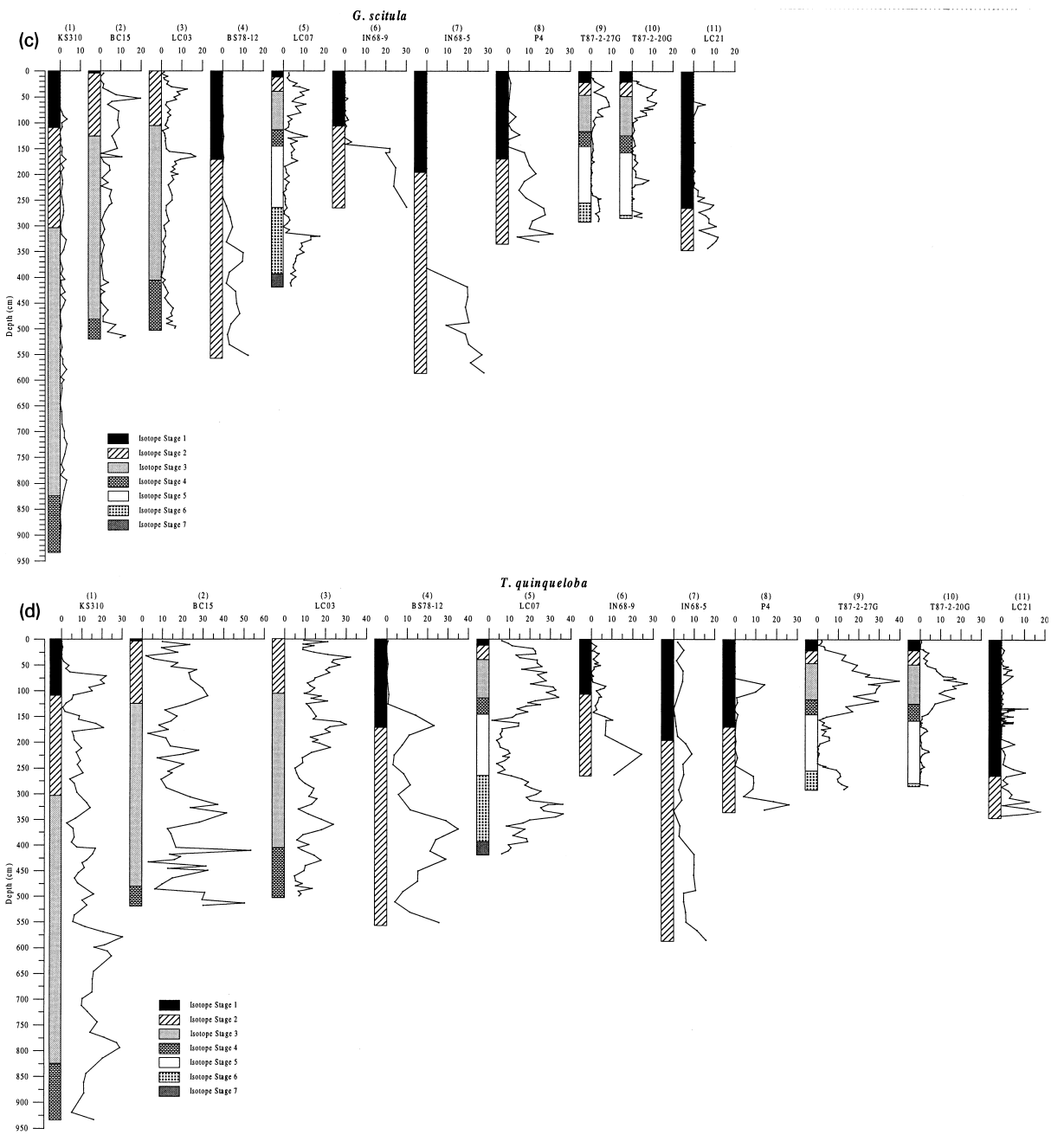

Fig. 4 (continued).

derma. This result is very similar to that of Thunell (1978) and Rohling et al. (1993), which is remarkable considering the high proportion of new western Mediterranean data incorporated into our analysis. Similar to Thunell (1978) and Rohling et al. (1993), we interpret our PC1 primarily as a sea surface temperature (SST) indicator, with increasing temperature for increasing scores on PC1.

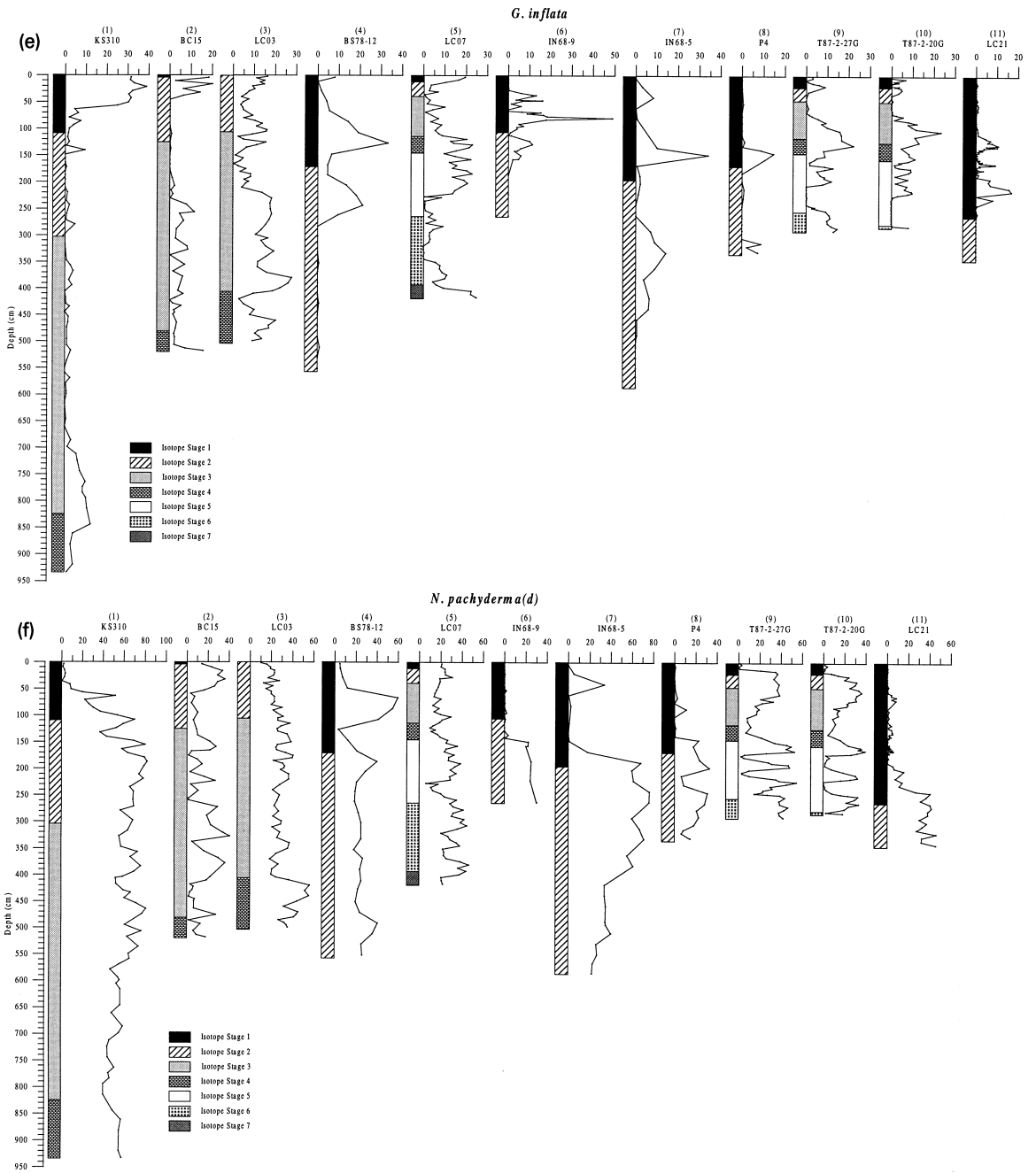

Fig. 4 (continued).

5. Discussion and conclusions

Although the faunal results show some surprising comparisons between geographically separated cores (see for example the *G. inflata* records of cores BC15, T87-2-20G and T87-2-27G), cores in between these sites record much less comparable signals. This comparison indicates that although planktonic

Table 3
Ranking of the species along the first PCA axis, together with their loadings

Species	PCA rankings
G. ruber	+0.55
SPRUDTS-group	+0.51
G. truncatulinoides	+0.003
G. bulloides	−0.07
G. glutinata	−0.12
G. scitula	−0.34
N. pachyderma	−0.35
G. quinqueloba	−0.39

foraminiferal biostratigraphy is a valuable correlation tool, it be must used on a local rather than a basin-wide scale to avoid misinterpretations. To enable detailed biostratigraphy for new cores, therefore, a data-base should be established of well-dated standard cores for each region, similar to, for example, the central Mediterranean last glacial maximum to Recent biostratigraphy of Jorissen et al. (1993). Similarly, biostratigraphy appears not to be possible on the basis of one single key species, as this might result in considerably diachronous correlations (see for example the deglacial exit of *G. scitula*; Fig. 4c). To avoid misinterpretations, the whole faunal assemblage should be taken into consideration. From the results of our transect it is immediately clear that correlation between the cores on wider, regional scales is both difficult and potentially misleading, unless additional independent dating tools are available. No sensible Mediterranean-wide high-resolution biostratigraphic framework seems conceivable, but a high potential remains for biostratigraphical dating of cores using area-specific foraminiferal assemblage variations.

With this pilot study, we hope to provoke further development of well-dated high-resolution biostratigraphic frameworks for the various sub-areas within the Mediterranean. In this manner, the difference between synchronous and diachronous faunal events may be quantified and so will provide new insight into palaeoceanographic developments in the basin.

The plot of scores per core on PC1 from our standardised Principal Component Analysis (Fig. 5) at first sight suggests a persistent general sea surface temperature (SST) gradient from west to east, cor-

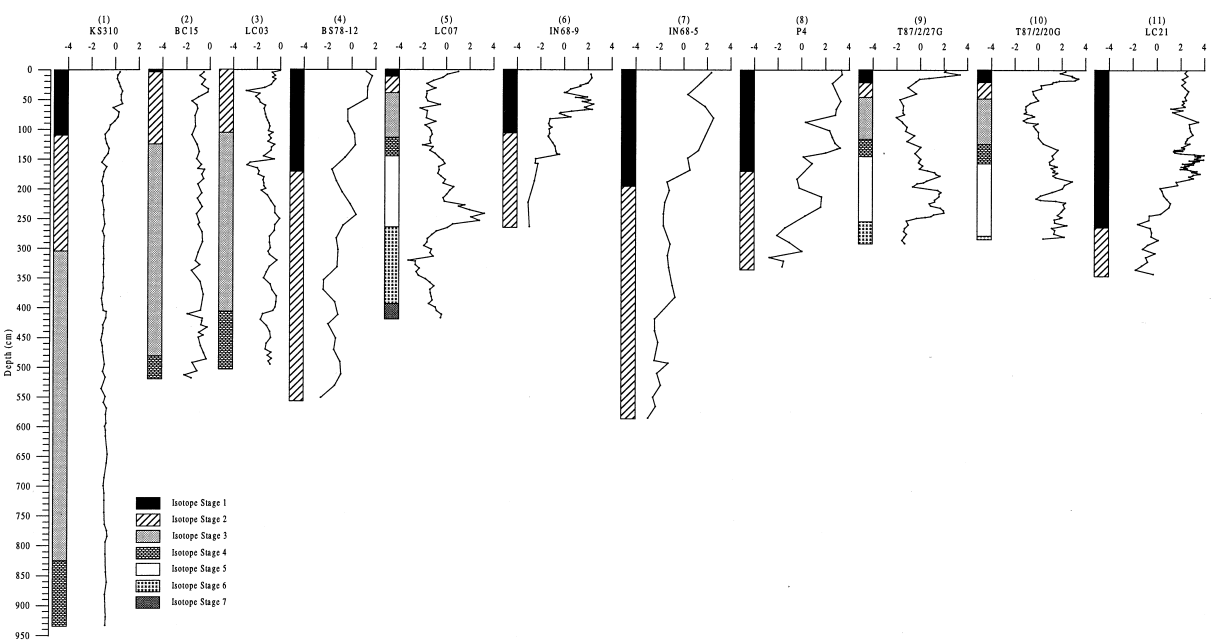

Fig. 5. Downcore scores from the principal component axis 1. Refer to Fig. 4 caption for oxygen isotope stage representation. Table 3 indicates the species dominating the positive or negative sides of the axis. Numbers in brackets refer to the core localities illustrated in Fig. 1.

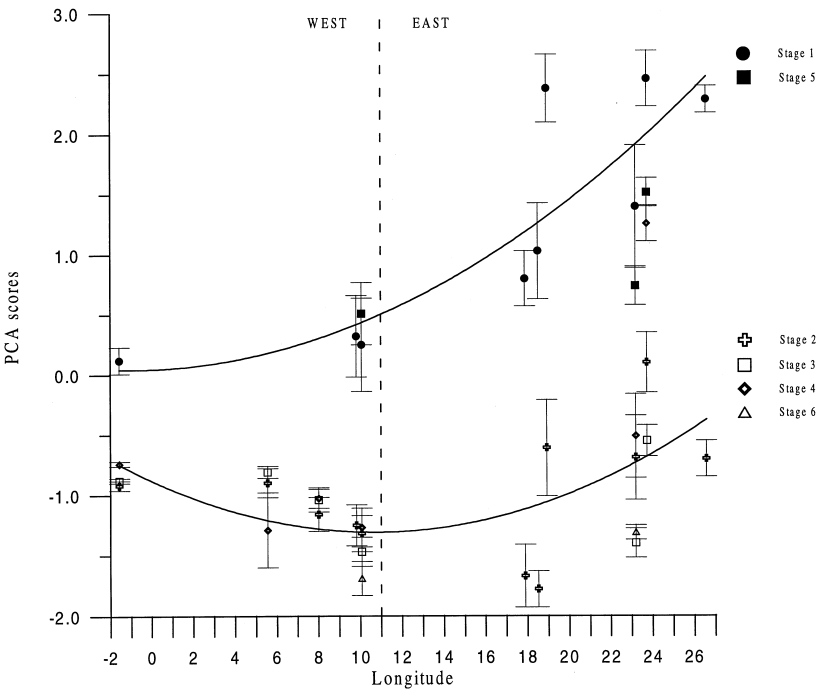

Fig. 6. A plot of the mean PCA scores versus longitude (see Table 1) for all the cores. The error bars are based on the mean standard error for each core. Black symbols refer to the interglacial stages whereas white symbols represent the glacial stages.

responding to the present-day observed SST trend (Wüst, 1961). Mean PCA scores per isotopic stage (Fig. 6), however, reveal differences in the W–E SST gradients between glacial and interglacial isotopic stages. Firstly, an obvious distinction appears between mean scores for glacial stages 2, 3, 4 and 6 and interglacial stages 1 and 5, as illustrated by the quadratic fits through these two associations. Admittedly, the quadratic fit ($R^2 = 0.74$) through the interglacial values is not significantly different from a linear fit, but it is used for easier comparison with the fit through the glacial values. The quadratic fit through the glacial values is weak, $R^2 = 0.34$ (linear would only be 0.09), but markedly better fits are obtained only when 5th or higher order polynomials are used which is not warranted by the quality of the data. The offset between the interglacial (higher) and glacial (lower) values is, as expected due to the reduction in SST values generally during glacial times.

Secondly, the interglacial values illustrate a straightforward SST increase from the Alboran Sea in the west to the Levantine Sea in the east, whereas the data for the glacial stages depict an initial SST decrease from the Alboran Sea to the central Mediterranean and a subsequent increase towards the east. Notably 'cold' values appear in the full glacial (stage 2) Aegean and Adriatic seas, suggesting that these northern basins formed the coldest parts of the glacial eastern Mediterranean, as is the case also today. The SST difference between the Adriatic and eastern Mediterranean at glacial times does not seem to have been very different from that during interglacial stages, whereas the Aegean Sea appears to have undergone relatively stronger glacial cooling.

Our PCA result confirms the observation of Rohling et al. (1993) that the sign of the temperature gradient in the eastern Mediterranean was the same at glacial times as it is today. Also, we find that the magnitude of glacial SST gradients over the eastern basin was probably comparable to the present, even if the entire basin would have experienced generally lower SSTs than today. A possible exception would be the increased relative cooling during isotopic stage 2 in the Aegean Sea, which requires validation

through further study. In the western Mediterranean, the inferred SST changes are more complicated, with an apparently reversed gradient compared to the present. The entire western basin seems to have undergone substantial glacial cooling, the significance of which needs to be determined through further study.

Acknowledgements

We thank Colin Chilcott, Stable Isotope Laboratory at the University of Edinburgh for the stable isotope analyses on cores LC03 and 07, and M. Den Dulk, N. Ampstead, R. Hale, L. Fraser and T. Much for micropalaeontological analyses. Thanks also to G. Rothwell (Mast-2 program PALEOFLUX) for access to cores LC03, 07 and 21, and to C. Vergnaud-Grazzini and C. Pujol for access to KS310. This study is supported by Mast-3 program Climatic Variability of Mediterranean Paleo-Circulation (CLIVAMP; MAS3-CT95-0043) and Southampton University grant A94/18, and contributes to UNESCO–IUGS program Climates in the Past (CLIP).

References

Buckley, H.A., Johnson, L.R., Shackleton, N.J., Blow, R.A., 1982. Late glacial to recent sediment cores from the eastern Mediterranean. Deep-Sea Res. 29, 739–766.

Cita, M.B., Chienici, M.A., Ciarupo, G., Moncharmont Zei, M., d'Onofrio, S., Ryan, W.B.F., Scorziello, R., 1973. Quaternary record in the Ionian and Tyrrhenian basins of the Mediterranean Sea. Init. Rep. Deep Sea Drill. Proj. 13, 1263–1339.

Cita, M.B., Vergnaud-Grazzini, C., Robert, C., Chamley, H., Ciaranfi, N., d'Onofrio, S., 1977. Palaeoclimatic record of a long deep sea core from the eastern Mediterranean. Quat. Res. 8, 205–235.

Ganssen, G., Troelstra, S.R., 1987. Paleoenvironmental changes from stable isotopes in planktonic foraminifera from eastern Mediterranean sapropels. Mar. Geol. 75, 221–230.

Herman, Y., 1972. Quaternary eastern Mediterranean sediments: micropalaeontological climatic record: In: Stanley, D.J. (Ed.), The Mediterranean Sea. Dowden, Hutchinson and Ross, Stroudsburg, PA, pp. 129–147.

Jorissen, F.J., Asioli, A., Borsetti, A.M., Capotondi, L., De Visscher, J.P., Hilgen, F.J., Rohling, E.J., Van der Borg, K., Vergnaud-Grazzini, C., Zachariasse, W.J., 1993. Late Quaternary central Mediterranean biochronology. Mar. Micropaleontol. 21, 169–189.

Kullenberg, B., 1952. On the salinity of the water contained in marine sediments. Medd. Oceanogr. Inst. Göteborg 21, 1–38.

Martinson, D.G., Pisias, N.G., Hays, J.D., Imbrie, J., Moore Jr., T.C., Shackleton, N.J., 1987. Age dating and the orbital theory of the ice ages: Development of a high-resolution 0 to 300,000-year chronostratigraphy. Quat. Res. 27, 1–29.

Muerdter, D.R., Kennett, J.P., 1984. Late Quaternary planktonic foraminiferal biostratigraphy, Strait of Sicily, Mediterranean Sea. Mar. Micropaleontol. 8, 339–359.

Olaussen, E., 1960. Descriptions of sediment from the Mediterranean and Red Sea. Rep. Swed. Deep-Sea Exped., 1947–1948 8 (5), 287–334.

Olaussen, E., 1961. Studies of deep sea cores. Rep. Swed. Deep-Sea Exped., 1947–1948 8 (6), 353–391.

Parker, F.L., 1958. Eastern Mediterranean foraminifera. Rep. Swed. Deep-Sea Exped., 1947–1948 8 (2), 217–283.

Paterne, M., Guichard, F., Labeyrie, J., Gillot, P.Y., Duplessy, J.C., 1986. Tyrrhenian Sea tephrochronology of the oxygen isotope record for the past 60,000 years. Mar. Geol. 72, 259–285.

Pujol, C., Vergnaud-Grazzini, C., 1989. Palaeoceanography of the last deglaciation in the Alboran Sea (western Mediterranean). Stable isotopes and planktonic foraminiferal records. Mar. Micropaleontol. 15, 253–267.

Pujol, C., Vergnaud-Grazzini, C., 1995. Distribution patterns of live planktic foraminifers as related to regional hydrography and productive systems of the Mediterranean Sea. Mar. Micropaleontol. 25, 187–217.

Rohling, E.J., De Rijk, S., 1999. Holocene climate optimum and Last Glacial Maximum in the Mediterranean: the marine oxygen isotope record. Mar. Geol. 153, 57–75.

Rohling, E.J., Gieskes, W.W.C., 1989. Late Quaternary changes in Mediterranean Intermediate Water density and formation rate. Paleoceanography 4, 531–545.

Rohling, E.J., Jorissen, F.J., Vergnaud-Grazzini, C., Zachariasse, W.J., 1993. Northern Levantine and Adriatic Quaternary planktic foraminifera; reconstruction of paleoenvironmental gradients. Mar. Micropaleontol. 21, 191–218.

Rohling, E.J., den Dulk, M., Pujol, C., Vergnaud-Grazzini, C., 1995. Abrupt hydrographic changes in the Alboran Sea (western Mediterranean) around 8000 yrs BP. Deep-Sea Res. 42, 1609–1619.

Rohling, E.J., Jorissen, F.J., De Stigter, H.C., 1997. 200 year interruption of Holocene sapropel formation in the Adriatic Sea. J. Micropaleontol. 16, 97–108.

Stuiver, M., Braziunas, T.F., 1993. Modelling atmospheric C-14 influences and C-14 ages of marine samples to 10,000 yrs BC. Radiocarbon 35 (1), 137–189.

Stuiver, M., Reimer, P.J., 1993. Extended C-14 data-base and revised Calib 3.0 C-14 age calibration program. Radiocarbon 35 (1), 215–230.

Tang, C.M., Stott, L.D., 1993. Seasonal salinity changes during Mediterranean sapropel deposition 9000 years B.P.: evidence from isotopic analyses of individual planktonic foraminifera. Paleoceanography 8, 473–493.

Thunell, R.C., 1978. Distribution of recent planktonic foraminifera in surface sediments of the Mediterranean Sea. Mar. Micropaleontol. 3, 147–173.

Thunell, R.C., Williams, D.F., 1983. Paleotemperature and paleosalinity history of the eastern Mediterranean during the late

Quaternary. Palaeogeogr., Palaeoclimatol., Palaeoecol. 44, 23–39.

Thunell, R.C., Williams, D.F., Kennett, J.P., 1977. Late Quaternary paleoclimatology, stratigraphy and sapropel history in eastern Mediterranean deep-sea sediments. Mar. Micropaleontol. 2, 371–388.

Todd, R., 1958. Foraminifera from western Mediterranean deep-sea cores. Rep. Swed. Deep-Sea Exped., 1947–1948 8 (3), 169–215.

Vazquez, A., Zamarreño, I., Reyes, E., Linares, J., 1991. Late Quaternary climatic changes on the southwestern Balearic slope (Western Mediterranean): isotopic, faunal, and mineralogical relationships. Palaeogeogr., Palaeoclimatol., Palaeoecol. 81, 215–227.

Vergnaud-Grazzini, C., Ryan, W.B.F., Cita, M.B., 1977. Stable isotopic fractionation, climatic change and episodic stagnation in the eastern Mediterranean during the Late Quaternary. Mar. Micropaleontol. 2, 353–370.

Wüst, G., 1961. On the vertical circulation of the Mediterranean Sea. J. Geophys. Res. 66, 3261–3271.